

Numerical Modeling of Fire Spread through Trees and Shrubs¹

William E. Mell*, Samuel L. Manzello, and Alexander Maranghides
*Building and Fire Research Laboratory, National Institute of Standards and Technology,
100 Bureau Drive, Gaithersburg, MD 20899 USA*

*Corresponding author: +301-975-4797 (office), email: ruddy@nist.gov

Abstract:

Keywords: fire, wildfire, CFD, numerical combustion, wildland fuel

1. INTRODUCTION

Vegetative fuels and fires in a wildland setting can be categorized into ground, surface, or crown types (e.g., Chap. 4 in Johnson and Miyanishi (2001)). The focus of this work is to develop a validated, physics-based, numerical model for simulating fire spread through trees (crown fuel type) and shrubs (surface or crown fuel type, depending on the height of the shrub). From a modeling point of view a distinguishing feature of fires is the flame height above the vegetative fuel bed. In fires with flame heights that are significantly larger than the height of the fuel bed most flaming combustion will take place above the fuel bed. This can occur, for example, in many grass fires. In such scenarios, there is some justification for using separate computational grids for the fire plume and the vegetation. This is especially useful for simulations over large domains (100s of meters on a side) since computational costs can be reduced. Such an approach was implemented recently and applied to Australian grassland fuels (Mell et al., 2006a). However, in scenarios where the fire plume is of the same scale as the fuel bed height, or the fire bed is of the same scale as fuel bed inhomogeneities, another approach is required in order to more fully capture the interaction between the fire and the vegetative fuels. Such scenarios can include fire spread through vegetation arrays of vertically arranged surface, mid-storey, and crown fuels each with varied fuel loading – especially during the initial stage of vertical flame spread for fires that ignite near the base of the vegetation and spread upward. This includes changes in the horizontal distribution of fuels (clumping or spottiness). Such variations in fuel loading are important considerations in devising fuel treatments, assessing the fire intensity of a prescribed fire, and assessing fire risk in wildland-urban interface (WUI). Fuels in the WUI are inherently inhomogeneous with a mixture of structural fuels and indigenous as well as ornamental vegetation. The work reported here, and in a separate paper at this conference which focused on firebrands generated by vegetation (Manzello *et al.*, 2006), is part of an effort by the National Institute of Standards and Technology (NIST) to develop a better understanding of fire behavior in the WUI. A webpage containing an overview of the project is available (Mell *et al.*, 2006b).

¹ Official contribution of the National Institute of Standards and Technology, not subject to copyright in the United States of America.

2. DESCRIPTION OF NUMERICAL MODEL

The numerical model is called WFDS for (Wildland-urban interface Fire Dynamics Simulator) and is based on FDS (Fire Dynamics Simulator) a fire behavior model developed at NIST for simulating structural and outdoor fires (e.g., pool fires, tank farm fires). FDS uses the methods of computational fluid dynamics (CFD) to solve the equations governing the fluid motion, combustion, and heat transfer. Throughout the course of its development, experiments conducted in NIST's Large Fire Laboratory, and elsewhere, have been used to evaluate and further refine the modeling approach. FDS is used currently used by hundreds of fire protection engineers around the world. Both a technical manual (McGrattan, 2004) and a users guide (McGrattan and Forney, 2004) are available on the web and the program itself can be downloaded. A visualization package called Smokeview for FDS output has also been developed at NIST (Forney and McGrattan, 2004). The ongoing development of WFDS is an extension of FDS to outdoor fire spread and smoke transport problems that include vegetative and structural fuels and complex terrain. The targeted application area for WFDS is the simulation of fire spread through the wildland-urban interface. To date, the approach has been used to simulate grassland fires on flat terrain (Mell *et al.*, 2006a). The work described in this conference paper is the initial stage of WFDS development for simulating fire spread in raised vegetation such as trees and shrubs. Both Mell *et al.* (2006a) and the FDS technical manual (McGrattan, 2004) contain a detailed description of the gas-phase model equations. A large eddy simulation approach is used for modeling the buoyancy driven turbulent flow and a mixture fraction based method for the gas phase combustion. The numerical approach for solving the gas phase model equations is described in detail in McGrattan (2004).

The approach used to model the solid phase is similar to models used by previous researchers. In particular Albin (1985, 1986) presented similar model equations for one-dimensional heat transfer in a medium containing vegetation and air under an assumed heat flux due to an idealize fire shape. Albin's approach provided a fire spread rate but did not model the pyrolysis or char oxidation of the solid fuel. More recently similar models for the heat transfer with the vegetative fuel bed have been incorporated in CFD models, which include (to differing approximations) thermal degradation (pyrolysis and char oxidation) and gas-phase combustion, to obtain a more complete approach to predicting the transient behavior of the fire and its buoyant plume (for example Dupuy and Morvan, 2005; Linn *et al.*, 2002; Mell *et al.*, 2006). A review of these methods is given in Mell *et al.* (2006). The approach used here to model the burning vegetation is still under development and testing. The model equations for heat transfer within the vegetative fuel is similar to that presented in Mell *et al.* (2006) and Morvan and Dupuy (2004) both of which are also similar to model equations presented by Albin (1985).

The vegetative fuel is assumed to be composed of sub-grid thermally thin, optically black, fuel elements. Both convective and radiative heat transfer within the vegetation is accounted for, as is the drag of the vegetation on the airflow. In general, as the temperature of a vegetative fuel increases, first moisture is removed followed by pyrolysis (the generation of fuel vapors) and char oxidation. In the modeling approach used here the temperature equation for the fuel bed is solved assuming a two stage endothermic decomposition process (water evaporation followed by solid fuel pyrolysis). At this stage in the model development char oxidation is not accounted for. In a given fuel layer the virgin fuel dries and then undergoes pyrolysis until the solid mass remaining equals a specified mass of char. The mass of char is obtained from a measured char fraction of 25% for Douglas fir (char fraction is the mass of char divided by the initial mass of the virgin fuel).

At the time of writing this conference paper two different models for fuel gas production via pyrolysis are being tested:

- (I) Fuel mass flux is linearly dependent on the fuel temperature. This model was presented by Morvan and Dupuy (2004) and was used in WFDS grassland simulations (Mell *et al.*, 2006).
- (II) Fuel mass flux begins at the measured fuel temperature for which flame attachment is assumed to occur (320 C). The magnitude of the fuel mass flux depends on the computed net heat flux into the fuel element and a specified heat of vaporization which is determined by simulating the experiments.

Method (II) is being considered because it may require less computational grid resolution than method (I). This is an important consideration for application of WFDS to landscape scale fire spread problems. At this point in the model development method (I) has been used for the simulation of the tree burning experiments and method (II) for simulation of the shrub burning experiments.

2. DOUGLAS FIR TREE BURNS

2.1 Douglas Fir Experiments

The tree burning experiments reported here were conducted in NIST's Large Fire Laboratory (LFL). Douglas Fir was selected as the tree species for these experiments because it is readily available in local tree farms and is abundant in the Western United States of America where WUI fires are most prevalent (Pagni, 1993; Albini, 1983). Trees of two different heights were burned: approximately 2 m and 5 m. The trees were size selected from a local nursery, cut, and delivered to NIST. The trees were mounted on custom stands and allowed to dry. During the experiments no wind was imposed on the trees.

The moisture content of the tree samples was measured using a Computrac² moisture meter. Needle samples as well as small branch samples (three heights, four radial locations at each height) were collected for the moisture measurements. The measurements were taken on bi-weekly basis. The moisture content, determined on a dry basis, is given as:

$$\text{Moisture Content} = M = \frac{M_{wet} - M_{dry}}{M_{dry}} * 100 \quad (1)$$

where M_{wet} and M_{dry} are the mass of the tree samples before and after oven drying, respectively. At the time of the experiments tree moisture content varied from 10 % to 50 %. The total combined uncertainty in these measurements is estimated to be ± 10 %. More than 30 days of drying time was required to reach moisture content levels at or below 30 %.

Experimental measurements from nine 2 m tall Douglas Fir and three 5 m tall Douglas Fir were collected. In addition, the 2 m trees were split into two groups: one with $M \approx 50\%$ and $10\% \leq M \leq 20\%$. Moisture levels for the 5 m tall trees was $23\% \leq M \leq 31\%$. Additional experiments are planned for this summer with 5 m tall trees with moisture contents of $M \approx 50\%$. Table 1 gives a summary of the characteristics for the 2 m tall trees and Table 2 does the same for the 5 m tall trees. The trees were ignited using a custom igniter assembly specifically designed for these experiments. Two burners, one for each tree height, were used. A snapshot of the burner used for the 2 m trees is shown in Fig. 1. The 2 m tree ignitor was circular, with a diameter of 80 cm and a heat release rate of 30

² Certain commercial equipment are identified to accurately describe the methods used; this in no way implies endorsement from NIST

kW; the 5 m tree ignitor was hexagonal with a span of 122 cm and a heat release rate of 130 kW. The ignitors surrounded the trees at their base and were fueled with natural gas. Both digital still photography and standard color video (standard 30 frames per second) were used to record the ignition and burning process of the Douglas Fir trees. For some experiments firebrands were collected. The results of the firebrand study are reported in a separate paper presented at this conference (Manzello *et al.*, 2006).



Figure 1 Snapshot of ignition procedure used for the 2 m tall Douglas Firs.

Two different load cells were used in order to resolve the disparate initial mass loading for the two tree heights considered. The voltage from the load cells was recorded using custom data processing software as the trees burned.

Table 1: Experiments with 2 m tall Douglas Fir trees.

Test #	Crown Height m	Bole width m	Initial total mass kg	mass loss (Δm_{dry}) kg	M average (needles) %
1	2.3	1.7	13.6	2.7	48
2	2.3	1.8	15.0	3.1	50
3	2.2	1.8	11.9	3.2	49
4	2.3	1.7	8.1	3.4	20
5	2.1	1.7	8.3	4.0	17
6	2.1	1.7	9.5	4.8	14
7	2.0	1.5	11.2	3.7	10
8	2.0	1.7	11.3	3.9	12
9	2.1	1.4	9.5	3.8	10
Average	2.2	1.7		3.7 (all) 3.0 ($M=50$) 3.9 ($M=10-20$)	

Table 2: Experiments with 5 m tall Douglas Fir trees.

Test #	Crown Height m	Bole width m	Initial total mass kg	mass loss (Δm_{dry}) kg	M average (needles) %
2	4.5	3.4	67.2	21.4	31
3	4.5	3.0	53.7	18.1	23
4	4.5	2.3	52.9	17.0	23
Average	4.5	2.9		18.8	26

In both Table 1 and Table 2 the height is measured from the ground to the top of the tree crown, bole width is the horizontal distance spanned by the base of the crown, initial total mass is the mass of the entire tree (include moisture mass) just prior to ignition, the dry mass loss (Δm_{dry}) is obtained from the measured total mass loss, Δm_{total} by:

$$\Delta m_{dry} = \frac{\Delta m_{total}}{1 + M} \quad (2)$$

Note that Δm_{total} is not listed in Table 1 and Table 2 but includes mass loss from drying, the generation of fuel gases (i.e., pyrolysis), and char oxidation (smoldering). Determining Δm_{dry} from Eq.(2) assumes that the char mass is completely consumed, leaving ash of negligible mass. It is also assumed that the moisture of all consumed fuel equals the measured needle moisture.

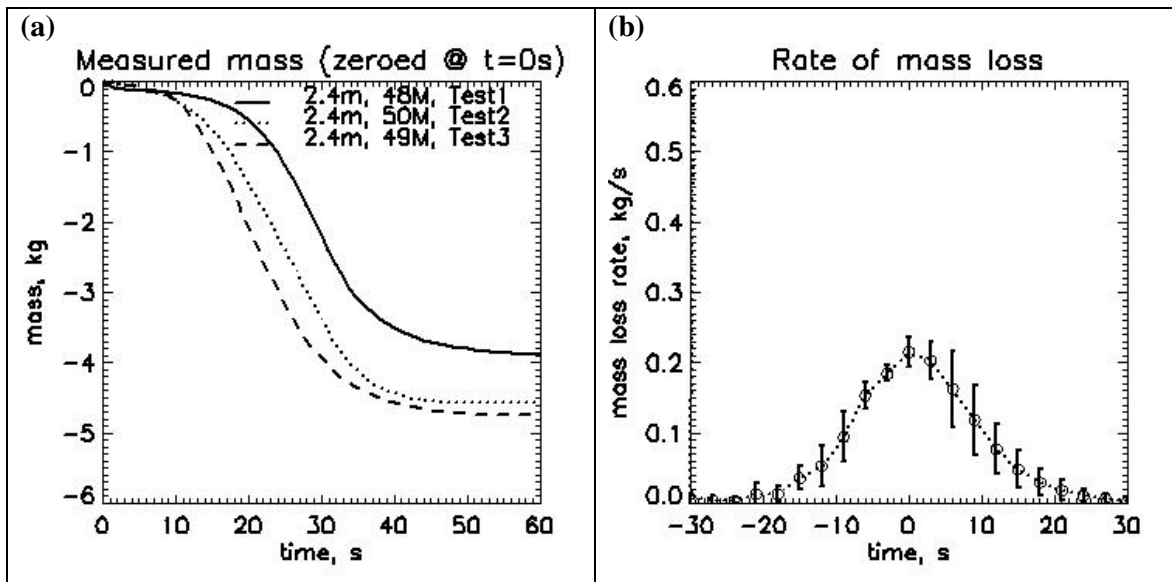


Figure 2 Experimental measurements from burning 2 m tall Douglas Fir trees with $M = 50\%$. **(a)** Time history of mass loss for each tree. The initial mass is shifted to zero at time 0 s for ease of comparison. See Table 1 for initial mass values. **(b)** Average mass loss rate versus time. Vertical bars show one standard deviation above and below the average mass burning rate for the three experiments.

Measured mass loss time histories from the experiments are plotted in Fig. 2(a) and Fig. 3(a) for the 2 m tall trees and Fig. 4(a) for the 5 m tall trees. The mass loss rate, with the peak mass loss rate shifted to time = 0 s, for the same cases are shown in Figs. 2(b), 3(b), and 4(b). The magnitude of the peak mass loss rate for trees with $M \approx 20\%$ increases by approximately a factor of five from the 2 m to the 5 m tall trees as can be seen by

comparing Fig. 3(b) and Fig. 4(b). Since the time interval over which the 2 m and 5 m tall trees burned was about the same (≈ 30 s), the total amount of dry fuel burned was also approximately a factor of five larger for the 5 m tall trees (see Table 1 and Table 2).

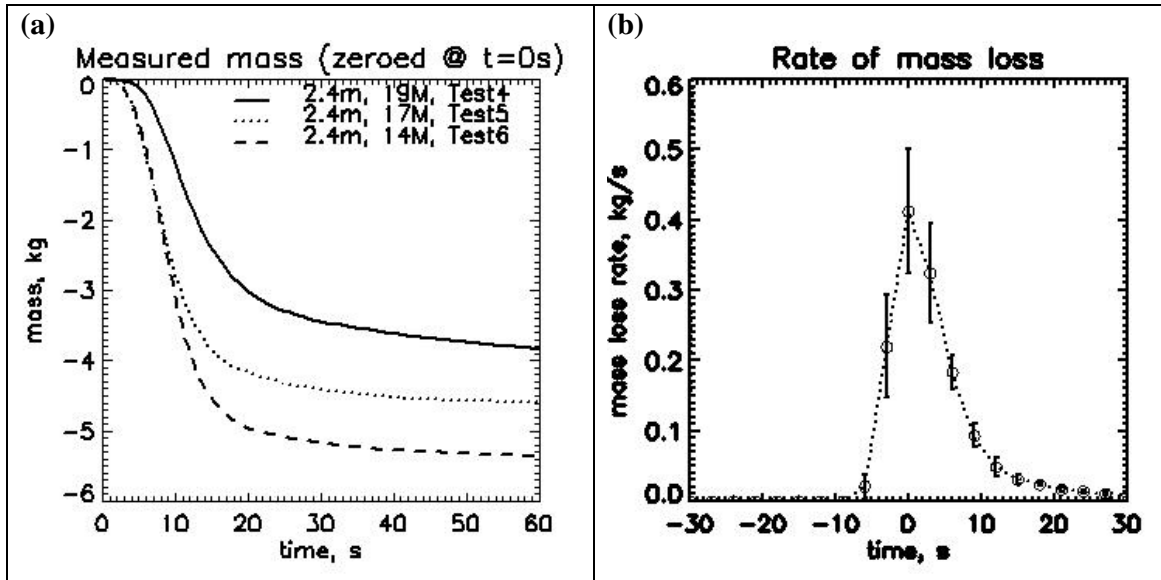


Figure 3 Experimental measurements for 2 m tall Douglas Fir. (a) Time history of mass loss for each tree with $M \approx 20\%$ (Tests 4-6 in Table 1). (b) Average mass loss rate versus time for Tests 4-9, $10\% \leq M \leq 20\%$ (see Table 1). Vertical bars show one standard deviation above and below the average mass burning rate for the six experiments.

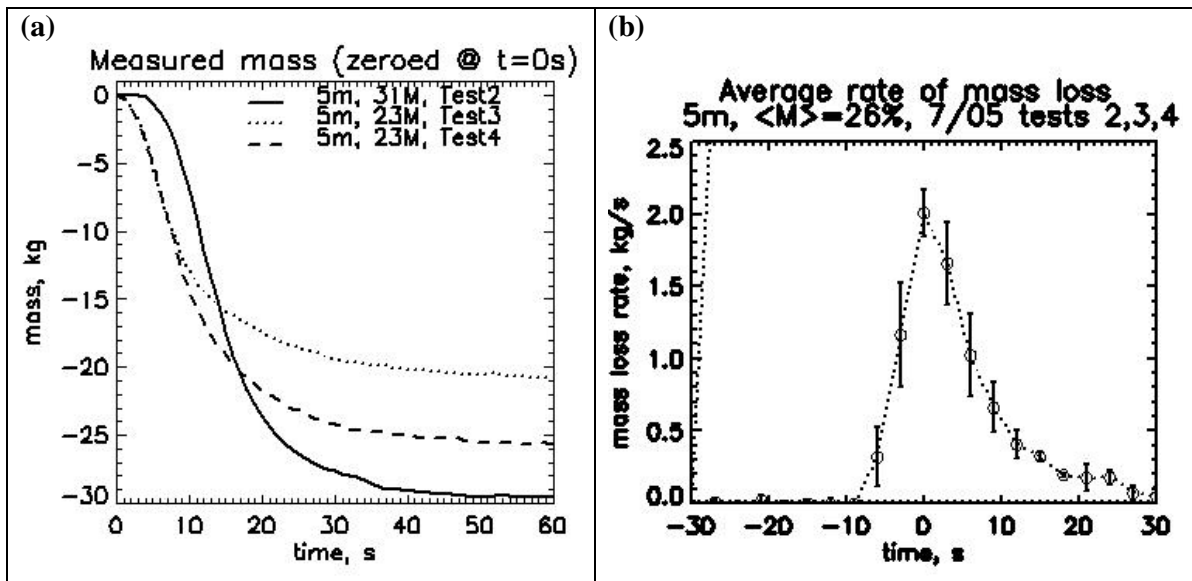


Figure 4 Experimental measurements for 5 m tall Douglas Fir. (a) Time history of mass loss. (b) Average mass loss rate versus time. Vertical bars show one standard deviation above and below the average mass burning rate for the three experiments.

2.2 Numerical Simulations of 2 m Douglas Fir Tree Burns

An example of numerical simulation and experimental results for a 2.4 m Douglas Fir is shown in Figure 5 below.

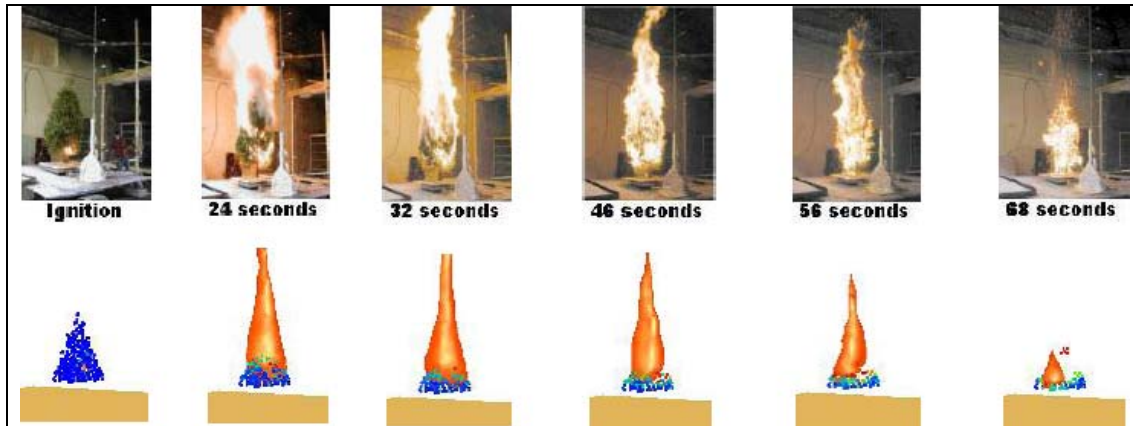


Figure 5 Snapshots of a burning 2.4 m tall Douglas Fir. Photographs of the tree burning in NIST's Large Fire Laboratory are along the top row. The bottom row shows the WFDS computer simulation of the burning tree as rendered by Smokeview (NIST's visualization tool for WFDS and FDS). The fuel is represented by points which are colored according to temperature (blue is ambient, red is pyrolysis). A surface of non-zero heat release rate is displayed in orange (approximates the location of the flame).

In the WFDS computer simulation the tree crown is approximated by a conical volume occupied by the thermally thin vegetative fuel elements. While it is possible to represent the tree crown to the resolution of the grid (7.5 cm) as a first step, and for simplicity, a cone shape crown is used. The average of the crown heights and base widths of the experimentally burned Douglas Firs are used to determine the height and base diameter of the cone shaped crown in the simulated tree (see Table 1 and Table 2). The model is capable of accounting for more than one type of thermally thin fuel element (e.g., needles and twigs). The fuel elements are subgrid and assumed to be uniformly distributed throughout the crown volume. A nonuniform distribution can be implemented but this would require knowledge of how the mass is distributed within the tree crown. For simplicity this was not done at the present time. Such non-uniformity of mass distribution may be important to fire dynamics through large tree crowns.

The trees were sampled to determine how much mass was present, in bulk, in the form of needles, twigs 0 to 3 mm, and twigs 3 to 6 mm in diameter. This distribution was approximately 70%, 15%, and 15% respectively. The surface to volume ratio (3900 1/m) of the needles was obtained by measuring the dimensions of the needles with calipers (accurate to 0.025 mm). The amount of thermally thin, dry, virgin fuel mass in the tree crown was determined by the measured mass loss and the pre-burn moisture content of the needles (3.9 kg for the 2 m and 18.8 kg for the 5 m trees). This mass value, along with the known conical volume, determines the bulk density of the dry fuel in the simulated tree (2.6 kg/m³ for the 2 m and 2.2 kg/m³ for the 5 m trees). A density of 514 kg/m³ was used for the fuel particle density (Ritchie, 1997). The heat of combustion is 17,700 kJ/kg which is the heat released per kg of gaseous fuel (*not* per kg of solid fuel) and was derived by averaging the Douglas Fir wood and foliage heat of combustion measurements of Susott (1987). The measured char fraction of twigs was 0.25 which agrees well with the measurements (0.21) of Susott (1982).

Ignition of the bottom of the tree crown was approximated by placing a ring of hot spots below the crown. The location of this ring matched that of the experimental burner (within the constraints of grid resolution) shown in Figure 1. Simulation results were sensitive to the ignition method (temperature and duration of hot spots). In the results shown here an ignition that had the least influence the subsequent burning of the tree crown was used.

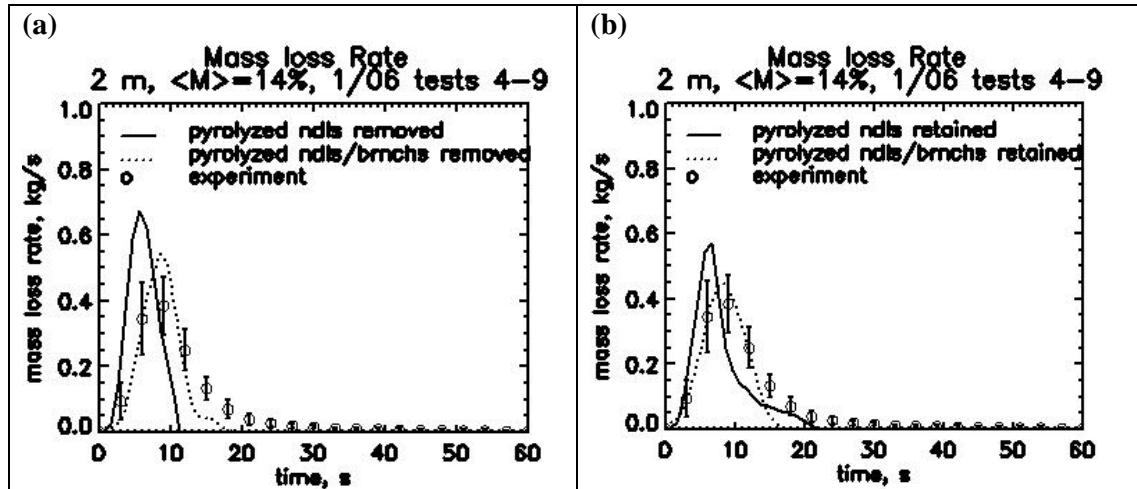


Figure 6: Time history of mass loss rate (kg/s) for the drier 2 m trees (test cases 4 – 9 in Table 1). The average of the experimentally measured mass loss rate is represented as circles with vertical range bars denoting one standard deviation above and below the average. **(a)** The vegetative fuel is represented as needles only (solid line) or by distributing the mass among three size bins based on bioassays of the trees: 70% as needles, 15% as twigs 0 mm to 3 mm in diameter, and 15% as twigs 3 mm to 6 mm in diameter (dotted line). For both cases the fuel element is removed once pyrolyzation is complete. **(b)** The vegetation is modeled as in (a) but the fuel elements are not removed once pyrolyzation is complete. Instead they remain as a source of drag and inert thermal mass.

Figure 6 shows the mass loss rate from the 2 m tree burning experiments and from WFDS simulations of the cone-shaped approximation of the experimental trees. The mass loss rate is a fundamental quantity that results from the coupled fire/fuel interaction as the fire spreads through the vegetation. Note that an estimate of the total heat release rate from the fire can be obtained by multiplying the mass loss rate by the heat of combustion. This is only an estimate because, for example, moisture mass loss contributes to the mass loss rate. The experimental data is plotted as circles for the average mass loss rate with vertical bars denoting the range of one standard deviation above and below the average. A number of WFDS simulations were run to explore sensitivities. The plotted simulations were on uniform computational grids with cubic grid cells 7.5 cm on a side in a 3 m by 3 m wide and 6 m tall domain (128,000 grid points); 45 cpu minutes were required for 30 s of simulated time on a current generation single processor computer. In Figure 6(a) two cases are shown. In the solid line case the vegetation consists only of needles. In the dotted line case the vegetation is distributed in three size bins (based on bioassay measurements): 70% needles, 15% twigs of diameter 0 – 3 mm, and 15% twigs of diameter 3 – 6 mm all with 14% moisture content. For both cases the vegetation is removed when pyrolysis is complete. WFDS predictions are somewhat improved when a more realistic mass distribution is used. In Figure 6(b) the same vegetation models are used but the pyrolyzed vegetation is not removed. Instead, it remains for the duration of the simulation as an inert

thermal mass (non-smoldering char) and a source of drag. Observations of the tree burns suggest that char oxidation was not significant until after flaming combustion ended. Retaining the drag presence of the vegetation resulted in some improvement of the model predictions. These issues are under ongoing investigation. The WFDS results plotted in Figure 6 (and below) should be viewed as representative of the performance of WFDS at an early stage of its development.

2.3 Numerical Simulations of 5 m Douglas Fir Tree Burns

The 5 m trees were also simulated using a cone shaped approximation to the tree crown.

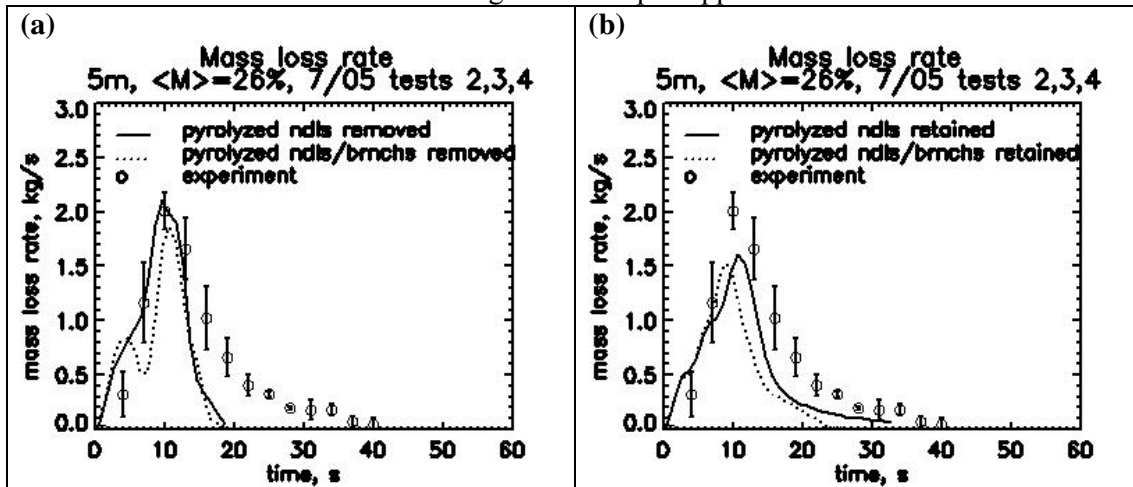


Figure 7: Mass loss rate time histories (kg/s) for the 5 m tall Douglas Firs. The average of the experimentally measured mass loss rate is represented as circles with vertical range bars denoting one standard deviation above and below the average. **(a)** The vegetative fuel is represented as needles only (solid line) or by distributing the mass among three size bins based on bioassays of the trees: 70% as needles, 15% as twigs 0 mm to 3 mm in diameter, and 15% as twigs 3 mm to 6 mm in diameter (dotted line). For both cases the fuel element is removed once pyrolyzation is complete. **(b)** The vegetation is modeled as in (a) but the fuel elements are not removed once pyrolyzation is complete. Instead they remain as a source of drag and inert thermal mass

Figure 7 shows the mass loss rate time histories for the 5 m tall Douglas Fir trees for the same model implementations as were plotted in Figure 6. There are clear differences in the behavior of WFDS for the different implementations. Retaining the vegetation fuel elements after they were completely pyrolyzed had more influence on the results (lowered the peak mass loss rate and extended its tail) than distributing the fuel mass across three size bins. Based on visual observation the cone approximation to the shape of the tree crown is likely to be less valid for these larger trees than for the 2 m trees. This is under investigation.

3. IDEALIZED SHRUB BURNS

3.1 Shrub Experiments

Dupuy *et al.* (2003) conducted a number of experiments in which a cylindrical wire mesh basket filled with *Pinus Pinaster* or excelsior was ignited along the bottom outer perimeter. To date, WFDS has been applied only to the *Pinus Pinaster* cases. The baskets were 20 cm tall and 20 cm, 28 cm, 40 cm in diameter. The bulk density was kept constant at 20 kg/m³. The measured *Pinus Pinaster* fuel moisture was 2%, char mass fraction was 0.25 to 0.30, surface-to-volume ratio was 4100 1/m, and fuel partial density was 640 kg/m³. The low

heat of combustion was 15,400 kJ/kg to 16,400 kJ/kg. Gas phase temperature, vertical velocity, mass loss rate, and the flame height were all measured. To date only simulated mass loss rates have been compared to experimental results. These experiments, while small in scale, are useful for model validation because the fuel is well characterized: only needles are present and they are homogeneously distributed in space.

3.2 Numerical Simulations of Shrub Burns

An example of a WFDS simulation of a 40 cm diameter idealized shrub experiment is shown in Figure 8.

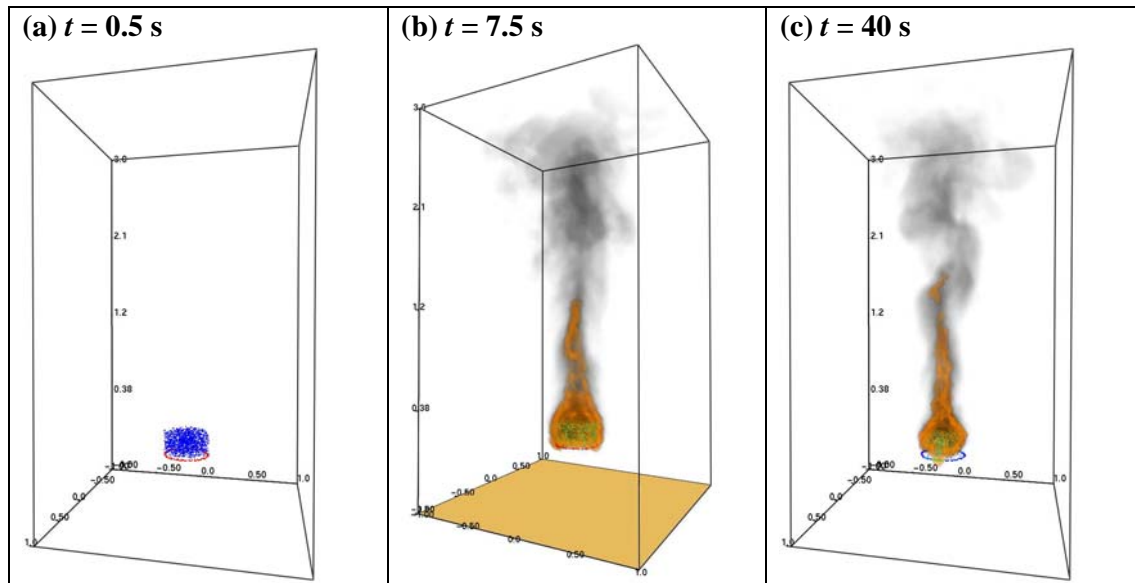


Figure 8: Snapshots of WFDS simulation of a idealized shrub burning experiment. The shrub is a cylinder 40 cm in diameter and 20 cm tall. Pinus pinaster fuel is shown as blue cylinder. The red ring beneath the shrub at $t = 0$ s is the active ignitor. The later snapshots show the heated shrub (non-blue colors), the approximation to the flame (orange), and smoke produced from combustion.

WFDS simulations of the idealized shrub use the material properties reported by Dupuy et al. (2003) and listed in the previous section. The heat of combustion is 15,600 kJ/kg and the char mass fraction is 27.5. The fuel consists of only Pinus Pinaster needles. As with the Douglas Fir simulations char oxidation was not modeled. Dupuy et al. (2003) note that significant char oxidation did not begin until after flaming had ended. This is consistent with retaining the needles as a source of drag after pyrolysis is complete.

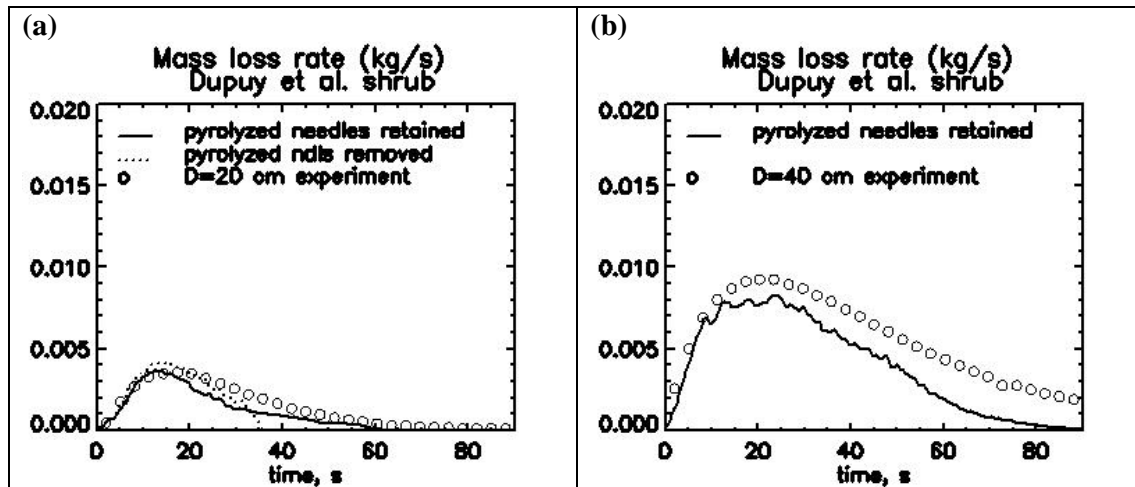


Figure 9: Time history of mass loss rate for two different sized idealized shrubs. Both experimental data (circles) and WFDS predictions (lines) are plotted. (a) Shrub of 20 cm diameter. (b) Shrub of 40 cm diameter.

Figure 9 shows the mass loss rate time histories as measured in the experiments (circles) and predicted by WFDS for two different sized cylindrical “shrubs”. Results for the $D = 20$ cm diameter shrub are shown in Figure 9(a) and the $D = 40$ cm shrub in Figure 9(b). Retaining the needles after pyrolysis is complete results in better predictions of the behavior of the tail of the time history curve, as can be seen in Figure 9(a). Note that the $D = 20$ cm case has a peak mass loss rate that is over two orders of magnitude smaller than in the 5 m tall Douglas Fir experiments (compare Figure 9(a) to Figure 7(a)). The shrub simulations require a smaller computational grid both because the size of the fuel source is smaller and the increased bulk density of the fuel (20 kg/m^3 for the shrubs compared to 2.6 kg/m^3 for the 2 m trees) results in larger gradients in heat flux (both convective and radiative). The computational grid used to in the Figure 9 simulations was uniform with cubic grid cells 2 cm on a side in a 1 m by 1 m wide and 2.4 m tall domain (300,000 grid points); 4.3 cpu hours were required for 30 s of simulated time on a current generation single processor computer.

4. SUMMARY

A set of Douglas Fir tree burning experiments conducted in NIST’s Large Fire Laboratory were performed in the last year. An overview of these experiments, which are still ongoing, was provided along with some experimental measurements. These experiments involved trees of approximately 2 m and 5 m heights. Two different moisture levels were considered for the 2 m tall trees. Additional experiments with 5 m tall trees at the higher moisture level will be conducted this summer.

A computer simulation model called WFDS (Wildland-urban interface Fire Dynamics Simulator) is currently under development at NIST. The tree burning experiments are being used to validate WFDS which is a time dependent, three-dimensional, physics-based modeling approach.

WFDS was used to simulate to the Douglas Fir tree burn experiments conducted at NIST and a set of experiments conducted by Dupuy *et al.* (2003) in which an idealized shrub was burned. The performance at this early stage of WFDS development and testing is

encouraging. Mass burning rates were reasonably well predicted. Further development and evaluation of WFDS is underway. Interested readers are encouraged to visit the webpage Mell *et al.* (2006b) for the most current developments. Once the WFDS is sufficiently well validated using results from controlled experiments, such as those described here, it will be applied and tested for more realistic problems such as the International Crown Fire Experiments (Stocks *et al.*, 2004).

5. ACKNOWLEDGEMENTS

Helpful discussions with Dr. Ronald Rehm of NIST and Russell Parsons of the United States Forest Service are gratefully acknowledged.

6. REFERENCES

- Albini, F.A. 1983 "Transport of firebrands by line thermals," *Comb. Sci. Tech.*, 32: 277-288.
- Albini, F.A. 1985 "A model for fire spread in wildland fuels by radiation," *Combust. Sci. and Tech.*, 42: 229-258.
- Albini, F.A. 1986 "Wildland fire spread by radiation -- a model including fuel cooling by natural convection," *Combust. Sci. and Tech.*, 45: 101-113.
- Dupuy, J-L, Marechal, J., Morvan, D. 2003 "Fires in a cylindrical forest fire burner: combustion dynamics and flame properties," *Combust. Flame*, 135:54-76.
- Dupuy, J-L, Morvan, D. (2005) "Numerical study of a crown fire spreading toward a fuel break using a multiphase physical model," *International Journal of Wildland Fire*, 14: 141-151.
- Forney, G.P. and McGrattan, K.B. 2004 "User's Guide for Smokeview Version 4: A Tool or Visualizing Fire Dynamics Simulation Data", NISTIR Special Publication, 1017, <http://fire.nist.gov/bfrlpubs/>
- Johnson, E.A. and Miyanishi, K., 2001. "Forest Fires: Behavior and Ecological Effects", Academic Press.
- Linn, R, Reisner, J., Colman, J.J. and Winterkamp, J. 2002 "Studying wildfire behavior using FIRETEC," *Intl. J. of Wildland Fire*, 11: 233-246.
- Manzell, S. L., Maranghides, A., Mell, W.E., Cleary, T.G. and Yang, J.C, 2006. "Firebrand Production from Burning Vegetation", Fifth International Conference on Forest Fire Research, November 27-30, 2006, Coimbra, Portugal.
- McGrattan, K.B. 2004 "Fire Dynamics Simulator (Version 4), Technical Reference Guide", NISTIR Special Publication 1018, McGrattan, K., editor, <http://fire.nist.gov/bfrlpubs/>
- McGrattan, K.G. and Forney, G. 2004 "Fire Dynamics Simulator (Version 4), Users Guide", NISTIR Special Publication 1019, <http://fire.nist.gov/bfrlpubs/>
- Mell, W.E., Jenkins, M.A., Gould J., Cheney, P., 2006a. "A Physics-Based Approach to Modeling Grassland Fires", *International Journal of Wildland Fire*, in press. http://www2.bfrl.nist.gov/userpages/wmell/PAPERS/GRASSFIRE_2006/wf06002_mell_et_al_grassfire_revised.pdf
- Mell, W.E., Manzello, S.L., Maranghides, A., Rehm, R. 2006b "Wildland Urban Interface and Wildland Fires: An Overview of the NIST WUI Project," <http://www2.bfrl.nist.gov/userpages/wmell/public.html>
- Morvan, D. and Dupuy, J.L. 2004 "Modeling the propagation of a wildfire through a Mediterranean shrub using a multiphase formulation,"

- Pagni, P. 1993 "Causes of the 20th October Oakland Hills conflagration," *Fire Safety Journal*, 21: 331-340.
- Ritchie, J.R., Steckler, K.D., Hamins, A., Cleary, T.G., Yang, J.C., Kashiwagi, T. 1997 "The effect of sample size on the heat release rate of charring materials," pp. 177-188, *Proceedings 5th Intl. Assoc. Fire Safety Science*.
- Susott, R.A. 1982 "Characterization of the thermal properties of forest fuels by combustion gas analysis," *Forest Sci.*, 23: 404-420.
- Stocks, B.J., Alexander, M.E., and Lanoville, R.A. 2004 "Overview of the International Crown Fire Modelling Experiment (ICFME)," *Can. J. For. Res.*, 34